Collaborative Mapping of an Earthquake-Damaged Building via Ground and Aerial Robots*

Nathan Michael, Shaojie Shen, Kartik Mohta, Yash Mulgaonkar, Vijay Kumar
GRASP Laboratory
University of Pennsylvania
Philadelphia, PA 19104-3409
{nmichael,shaojie,kmohta,yashm,kumar}@grasp.upenn.edu

Keiji Nagatani, Yoshito Okada, Seiga Kiribayashi, Kazuki Otake, Kazuya Yoshida, Kazunori Ohno, Eijiro Takeuchi, Satoshi Tadokoro
Tohoku University
Sendai, Japan
{keiji,okada,seiga,otake,yoshida}@astro.mech.tohoku.ac.jp
{kazunori,takeuchi,tadokoro}@rm.is.tohoku.ac.jp

Abstract

We report recent results from field experiments conducted with a team of ground and aerial robots toward the collaborative mapping of an earthquake-damaged building. The goal of the experimental exercise is the generation of 3D maps that capture the layout of the environment and provide insight to the degree of damage inside the building. The experiments take place in the top three floors of a structurally compromised engineering building at Tohoku University in Sendai, Japan that was damaged during the 2011 Tohoku earthquake. We provide details of the approach to the collaborative mapping and report results from the experiments in the form of maps generated by the individual robots and collaboratively. We conclude by discussing observations from the experiments and future research topics.

1 Introduction

In this work we report recent results from field experiments conducted with a team of ground and aerial robots toward the mapping of an earthquake-damaged building. We focus on the investigation of the feasibility of deploying aerial robots, specifically a quadrotor, into disaster scenarios where the building is critically damaged but still accessible to robots and humans for experimental purposes. The experimental environment covered the top three floors of an engineering building on the campus of Tohoku University in Sendai, Japan during the first week of August, 2011. Representative images of the interior and exterior of the building are shown in Figs. 1-2.

On March 11, 2011, a 9.0-magnitude earthquake (on the moment magnitude scale) occurred off the coast of Japan, approximately 130 km from Sendai (Magnitude, 2011). The consequences of the earthquake were devastating with significant loss of human life and damage to the environment. Resulting tsunami waves generated further damage and instigated a meltdown at a nuclear power plant near Fukushima, Japan (Tabushi, 2011).

Several robotics research groups and companies responded to this natural and nuclear plant disaster (Nagatani et al.,

*This work builds upon a conference paper currently under review (Michael et al., 2012).

Figure 1: Panoramic images depicting the interior of the building. These images are representative of the clutter found throughout the experimental areas.

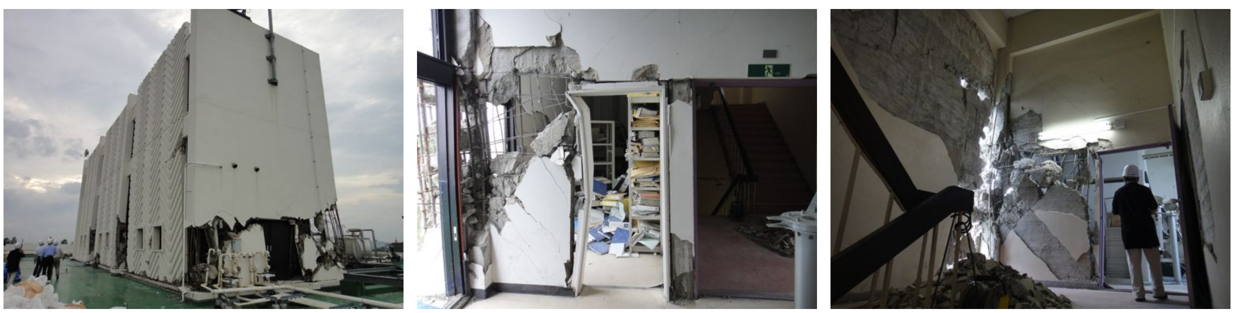

Figure 2: The building suffered significant structural damage due to the earthquake.

2011; Ackerman, 2011). Ground robots with onboard sensing enabled environmental observation of the compromised nuclear power plants in regions inaccessible to humans due to high levels of radioactivity. The ground robots were equipped with long-range cable tethers to enable remote communication, tele-operation, and the transmission of sensor data. These ground robots proved capable in maneuvering through the cluttered environments (Guizzo, 2011).

We are interested in exploring the possibility of leveraging an autonomous quadrotor in such environments through field experiments that focus on cooperative mapping using both ground and aerial robots. Aerial robots offer several advantages over ground robots including the ability to maneuver through complex three-dimensional environments and gather data from vantages inaccessible to ground robots. Further, quadrotors are able to hover in place, making them well-suited for observation and human-guided or autonomous inspection. However, aerial robots also suffer from several limitations that reduce their applicability in disaster scenarios such as the need for wireless communication and a limited onboard power supply which restricts the platform's payload capacity and flying time.

Given the prior experience of using ground robots at the nuclear power plant disaster site, we designed the experimental scenario based on conditions consistent with those found at the disaster site. Consider an earthquake-damaged building with multiple floors that are generally accessible to ground robots. However, various locations in the environment are inaccessible to the ground robots due to debris or clutter. The goal of the experimental exercise is the generation of 3D maps that capture the layout of the environment and provide insight to the degree of damage inside the building. Additionally, there may be specific regions of interest that require attention from operators during the mapping. Throughout the experiments, remote operators must be able to maintain control of the robotics platforms on the ground and in the air.

The experiment design highlights the need for heterogeneity. Ground robots do not suffer as greatly from the same payload limitations as quadrotors and are therefore able to carry larger sensor payloads, maintain tethered communication links, and operate for longer periods of time. However, quadrotors provide mobility and observational capabilities unavailable to ground robots. Hence, to build a rich 3D representation of the environment, we leverage the advantages of each platform and in doing so, mitigate the platform limitations.

The problems of localization and mapping in 3D environments are well-studied for both ground and aerial robots and many methodologies exist to address these problems. In this work, we focus primarily on the integration of our prior work in the areas of localization and mapping for ground and aerial robots. However, there are several examples of prior works employing similar methodologies to our own approach for either ground or aerial platforms (Pellenz et al., 2010; Bachrach et al., 2011) including cooperative mapping with ground and aerial platforms (Kim et al., 2010; How et al., 2009). Researchers have also pursued the mapping of complex environments for applications such as search and rescue via ground and aerial platforms (Murphy et al., 2009; Gonzalez et al., 2011; Pratt et al., 2008). Therefore, the contributions of this work are three-fold. First, it experimentally supports the argument that the mapping of complex multi-story environments with ground and aerial robots in disaster scenarios is viable (or nearly viable) given the current state-of-the-art in vehicle design, sensors, computation, and algorithms. Second, it supports the statement that the strengths and weaknesses of individual robot platforms may be overcome by employing heterogeneity in system design. Third, it provides insight into the gap between the current technological capabilities and the remaining challenges we must overcome toward application in true disaster scenarios.

2 Experiment Design and Methodology

To address the requirements of the experimental scenario, we use three different research platforms. The first platform is a ground robot equipped with an onboard sensing suite that enables the generation of dense 3D maps. The vehicle is tele-operated through the multi-floor environment while simultaneously collecting sensor data. After the operators identify locations in the environment that are inaccessible to the ground platform, a second ground platform equipped with an automated helipad is tele-operated to these locations and carries a quadrotor robot equipped with onboard sensing that is able to autonomously open and close the helipad and take-off and land from the helipad (Fig. 3). The aerial robot is physically transported by the ground robot to each location of interest where it autonomously takes-off before an operator is able to guide the robot to map or observe these inaccessible regions. Upon completion of the mapping and observation phase, the aerial robot is remotely signaled to autonomously land and close the helipad. The quadrotor is then guided to the next location of interest via the tele-operated ground robot.

The experiment primarily focuses on the problems of localization and cooperative mapping in 3D environments with ground and aerial robots. In this work, we do not emphasize vehicle autonomy as the experiments required that the operators tele-operate the vehicles. We discuss this requirement further in Sect. 4. During the experiments, tele-operation is conducted over wireless communication. However, we assume that in a disaster scenario, the ground vehicles will communicate with an external operator via a tether as currently employed at the Fukushima site (Nagatani et al., 2011). Communications with the aerial robot are via a local access point carried by the ground robot.

In this work, we leverage our previous efforts in the areas of ground robot design (Rohmer et al., 2010), sensor design for 3D map building (Ohno et al., 2008), and ground robot tele-operation (Okada et al., 2011) toward mapping with ground robots (Ohno et al., 2010; Ohno et al., 2009; Nagatani et al., 2008). Additionally, we build upon prior work towards autonomous navigation and 3D mapping with an aerial robot (Shen et al., 2011; Shen et al., 2012).

Figure 3: The Quince ground platform carries the Pelican aerial robot via a landing pad. The aerial robot opens and closes the landing pad via a wireless interface during autonomous take-off and landing. A video of the experiment is available at http://mrsl.grasp.upenn.edu/nmichael/jfr2012.mov.

(a) (b) (c)

Figure 4: The three robots used in the experiments include the Kenaf (Fig. 4(a)) and Quince (Fig. 4(b)) tracked ground robots. Here we see the Quince transporting the Pelican between discrete sites of interest via the landing pad (Fig. 4(c)).

2.1 Robot Platforms

As previously discussed, we employ three robot platforms for this work: two tracked ground platforms (Kenaf and Quince) and a quadrotor (Pelican). We now briefly detail each platform.

2.1.1 Ground Robots

The Kenaf is a tracked ground platform with an onboard rotating laser-scanner that provides feature-rich 3D point clouds of the environment (Fig. 4(a)). The laser scanner on the Kenaf operates at 40 Hz and rotates about the vehicle body-frame at 0.2 Hz. All laser scans from one revolution are assembled into a 3D point-cloud aligned with the robot body-frame origin. Further details of the platform and 3D laser scanner are available in (Ohno et al., 2010; Ohno et al., 2009) and (Ohno et al., 2008), respectively. The Quince platform (detailed in (Rohmer et al., 2010), Fig. 4(b)) shares a similar tracked design. Both platforms provide odometry information and are equipped with stabilizing tracked arms that permit climbing stairs and navigating clutter- or debris-filled environments.

The Kenaf and Quince provide visual information for the tele-operation of the vehicle including camera imagery of the surrounding environment during operation. We process any additional sensory information from the Kenaf and

Figure 5: The aerial robot flies through cluttered regions of the environment that are inaccessible to the ground robot and builds a 3D map that will be merged with the maps made by the ground robot.

Quince off-board.

For this work, we equipped the Quince with a landing pad that opens and closes via a remote signal transmitted over an 802.15.4 wireless interface (Fig. 4(c)). The landing platform is made of impact resistent ABS plastic. The structural integrity is provided by an underlying framework of slotted aluminum extrusions. The arms that robustly grip the base of the aerial robot are also fabricated from ABS and lined with dense foam to provide additional compliance and absorb vibrational or impulse forces on the vehicle due to the Quince going over rough terrain and steps. Two pairs of aluminum carriage-rail assemblies ensure that the arms remain parallel to each other throughout the deployment and retraction phase. The gripping arms are driven by linear actuators and the motion of the two arms is governed by limit switches to prevent over extension or retraction. The onboard processor controls the direction and braking of the two linear actuators and receives control commands via the wireless interface.

2.1.2 Aerial Robot

The Pelican quadrotor robot platform is sold by Ascending Technologies, GmbH (Ascending Technologies, GmbH,) and is equipped with an IMU (accelerometer, gyroscope, magnetometer) and pressure sensor. We developed custom firmware to run at the embedded level to address feedback control and estimation requirements. The other computation unit onboard is a 1.6 GHz Atom processor with 1 GB of RAM. The sensors on the robot include a Hokuyo UTM-30LX (laser), and a Microsoft Kinect sensor. A custom 3D printed mount is attached to the laser that houses mirrors pointing upward and downward. Communication with the robot for monitoring experiment progress and remote tele-operation is via an 802.11n access point mounted on the Quince.

Unlike the ground robots, the aerial robot requires some degree of onboard autonomy to permit autonomous navigation, take-off, and landing. Therefore, the vehicle must be able to localize its position based on the current environment map and address the planning and control considerations required to permit autonomous navigation, take-off, and landing during experimentation. The details of the algorithms employed to enable these capabilities are provided in (Shen et al., 2011; Shen et al., 2012). Figure 9 depicts a representative 3D map generated online during the experiments that is transmitted to the operator and used for autonomous navigation.

For this work, we require some degree of operator control to permit tele-operation of the vehicle. However, the complexity of the environment and the fact that the operator frequently did not have line-of-sight vision of the vehicle prevented full manual control of the vehicle. Therefore, we provided a "semi-autonomous" mode which permitted the operator to control the vehicle as a kinematic point-model agent or via waypoint control in the current map. Hence, at any moment, the operator could transition between full-autonomy and semi-autonomy to permit closer inspection of a location of interest or override the current behavior of the vehicle.

For this work, the autonomous take-off and landing is based on the originating position of the aerial robot in the current map. Therefore, we required that the Quince not move while the Pelican was flying. Although the autonomous landing

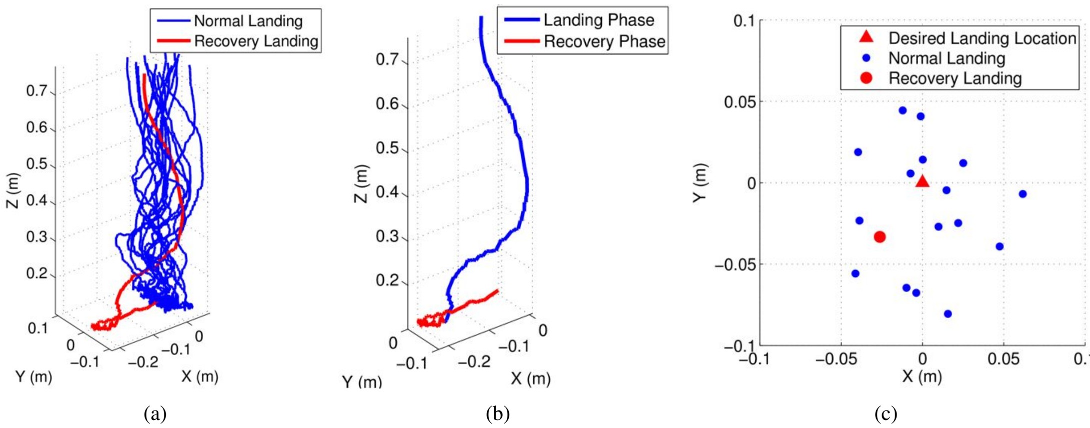

Figure 6: Partial trajectories of the aerial robot during seventeen landing trials (Fig. 6(a)). During one trial, the vehicle attempts and fails to land, causing it to enter a recovery phase before successfully landing (Fig. 6(b)). A scatter plot of the final landing locations is shown in Fig. 6(c).

maneuver was feed-forward in the sense that it did not observe the platform while landing, we found that vehicle was able to land without issue in general. However, the autonomous landing maneuver also included a recovery phase should the vehicle detect that it did not successfully land on the platform. This lack of additional feedback information was primarily due to the short time-frame in which these experiments needed to be conducted prior to the experimental site becoming unavailable.

The recovery phase of the autonomous landing is based on the position of the robot with respect to the desired landing location. The primary source of error during landing is due to the ground effects induced by the vehicle's proximity to the landing pad. If the error between the desired landing location and current vehicle state is within 2 cm in height but greater than 8 cm in either x or y directions, the vehicle will enter a recovery phase where it will attempt to regulate 1 cm above the desired landing location and concurrently estimate the changes in the dynamic model resulting from ground effects (as discussed in (Shen et al., 2011)). The landing pad is designed to accomodate landing deviations of up to 10 cm in the x and y directions.

We evaluated the performance of the system to establish a suitable level of performance, both in landing pad design and autonomous flight, to permit operation in a feed-forward manner as discussed above. Figure 6(a) depicts the performance of the vehicle over seventeen trials where the vehicle is asked to autonomously land from a variety of initial conditions, all an appreciable distance from the landing pad. Note that of these seventeen trials, only one requires that the vehicle attempt to recover (Fig. 6(b)). The mean of the error representing the distance between the intended landing location and actual landing location over the trials is on the order of 1 cm in x and y directions with the spread shown in Fig. 6(c).

2.2 Map Generation and Merging

We now briefly describe the methods used to generate the 3D maps during the experiment. The experiment consisted of two phases. During the first phase, we tele-operated the Kenaf across the three stories of the building and collected sensor data for 3D map generation. We also identified locations inaccessible to the vehicle (six in total). After completing the first mapping phase, the Quince carried the Pelican to the six locations across the three stories of the building to further extend the map.

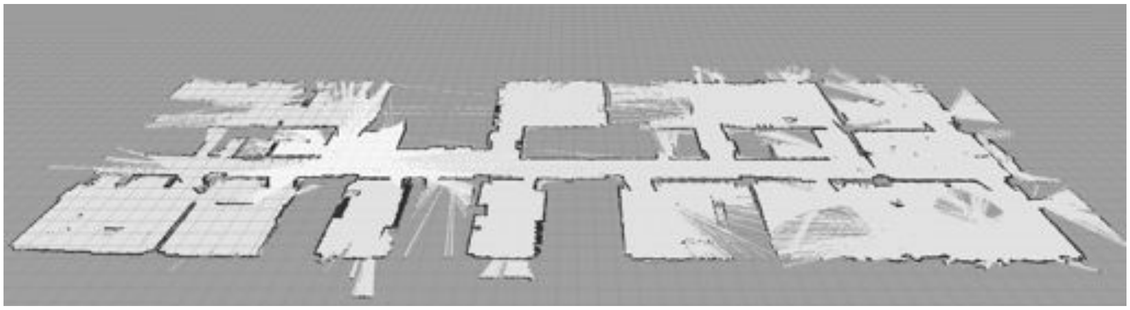

(a)

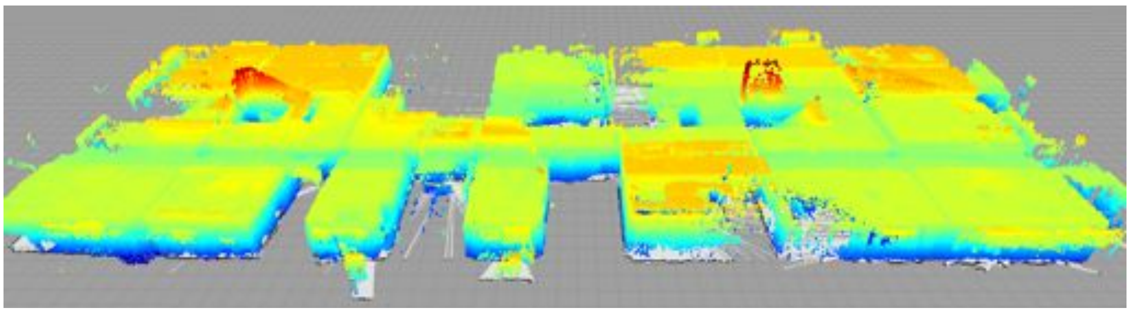

(b)

Figure 7: The 2D occupancy grid map (Fig. 7(a)) and 3D point-cloud map (Fig. 7(b)) of the 7th floor generated via the Kenaf sensor data.

2.2.1 Kenaf

We used two methods to generate 3D maps via the Kenaf sensor data. The first approach uses a 3D iterative closest point (ICP) algorithm to determine incremental body-frame transformations. Details of map generation via this method are discussed in (Ohno et al., 2009). However, as noted in our prior work, 3D ICP can converge to poor alignment solutions. We found that when the vehicle was operating on a level z-plane (i.e. not in stairwell), we could yield a more robust mapping solution by employing the methods discussed in (Shen et al., 2011) which requires the assumption that the environment is generally described by flat planes and vertical walls (the 2.5D assumption).

For this approach, map corrections are done on a per-revolution basis with the assumption that the odometry error within one revolution is sufficiently small and the assembled point-cloud is accurate. Figure 8 shows a typical point-cloud output from one revolution. The point-cloud is down-sampled via a voxel grid filter, from which we generate a 2D point-cloud by choosing all samples at a fixed z-height. We compute SLAM corrections from this 2D point-cloud and odometry data via the methods detailed in (Shen et al., 2011) to yield corrected robot poses. These corrected poses are used with the 3D point-clouds to generate globally consistent 3D maps of the environment (Fig. 7(b)) along with 2D occupancy grid maps resulting from the 2.5D assumption (Fig. 7(a)). In general, we applied the second method when operating on level terrain and only reached for 3D ICP-based SLAM methods when operating in the stairwell regions.

2.2.2 Pelican

As previously noted the Pelican generates a 3D map online during autonomous flight following the methodology detailed in (Shen et al., 2011). Unlike the Kenaf, the Pelican collects data at discrete locations in the environment with the origin associated with the take-off location as visited by the Quince. In a manner similar to above, we generate a

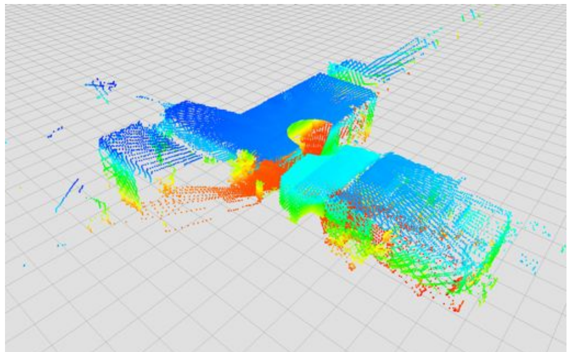

Figure 8: The 3D rotating laser scanner on the Kenaf generates feature-rich 3D point clouds. Here we show the full output from a single revolution of the scanner.

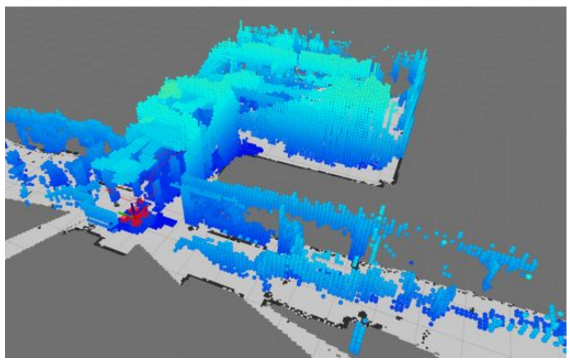

Figure 9: A representative 3D map generated by the aerial vehicle during flight. A 2D occupancy grid map is also generated at all times. The vehicle and its planned path are shown as a red mesh and line, respectively.

3D point-cloud and a 2D occupancy grid map associated with each take-off location. Figure 9 depicts a representative visualization of the sensor data and generated maps. These maps are merged with the Kenaf maps from the previous section to form a complete 3D representation of the environment.

2.2.3 Merging Ground and Aerial Robot Maps

We begin by registering the two maps (the Kenaf and Pelican maps) via an initialization point near the known take-off location of the Pelican, as the Quince visits locations defined in the Kenaf map. Further refinement between the two maps is accomplished via ICP. This approach is applied for each of the rooms visited by the Pelican.

3 Results

As previously noted, the goal of this work is the generation of 3D maps that capture the layout of the environment and provide insight to the degree of damage inside a multi-story building. In Figs. 10-11 we provide full 2D and 3D maps of the 7th-9th floors of the building. We can clearly see features in the environment, such as the structural braces placed on the 8th floor (Fig 11(d)) to prevent further structural collapse and the locations on the 9th floor (Fig. 10(c)) where the walls caved out of the building, leaving large openings. In Fig. 13, we show the 3D map for the stairwell between

(a) 7th Floor

(b) 8th Floor

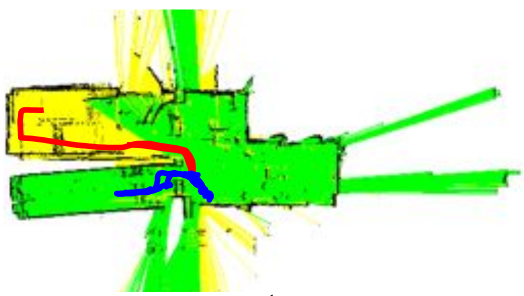

(c) 9th Floor

Figure 10: The 2D occupancy grid maps generated during the experiment of the 7th, 8th, and 9th stories of the Tohoku University Electrical Engineering Building. The contributions to the map made by the Kenaf are shown in yellow with an overlay of the contributions made by the Pelican in green. The path of the Quince is shown in red while the trajectory followed by the Pelican is depicted in blue.

the 7th and 8th floors at various z-height levels.

The experiment lasted a total of 2.5 hours with the Kenaf first generating a 3D map via tele-operation followed by the Quince carrying the Pelican to discrete locations. It is worth noting that while the flight-time of the Pelican in confined environments can be as low as 5 min, we only needed to replace the battery in the vehicle twice due to our use of the aerial robot only when necessary for map extension. Although our Pelican can traverse hallways and stairwells autonomously (as shown in (Shen et al., 2011)), we conserved the battery power whenever possible by employing the Quince.

4 Discussion, Conclusion, and Areas for Future Work

The original experiments were intended to occur over several days but we found that we were able to complete the full exercise in one afternoon without any failures. While the fact that we were able to map a multi-story building

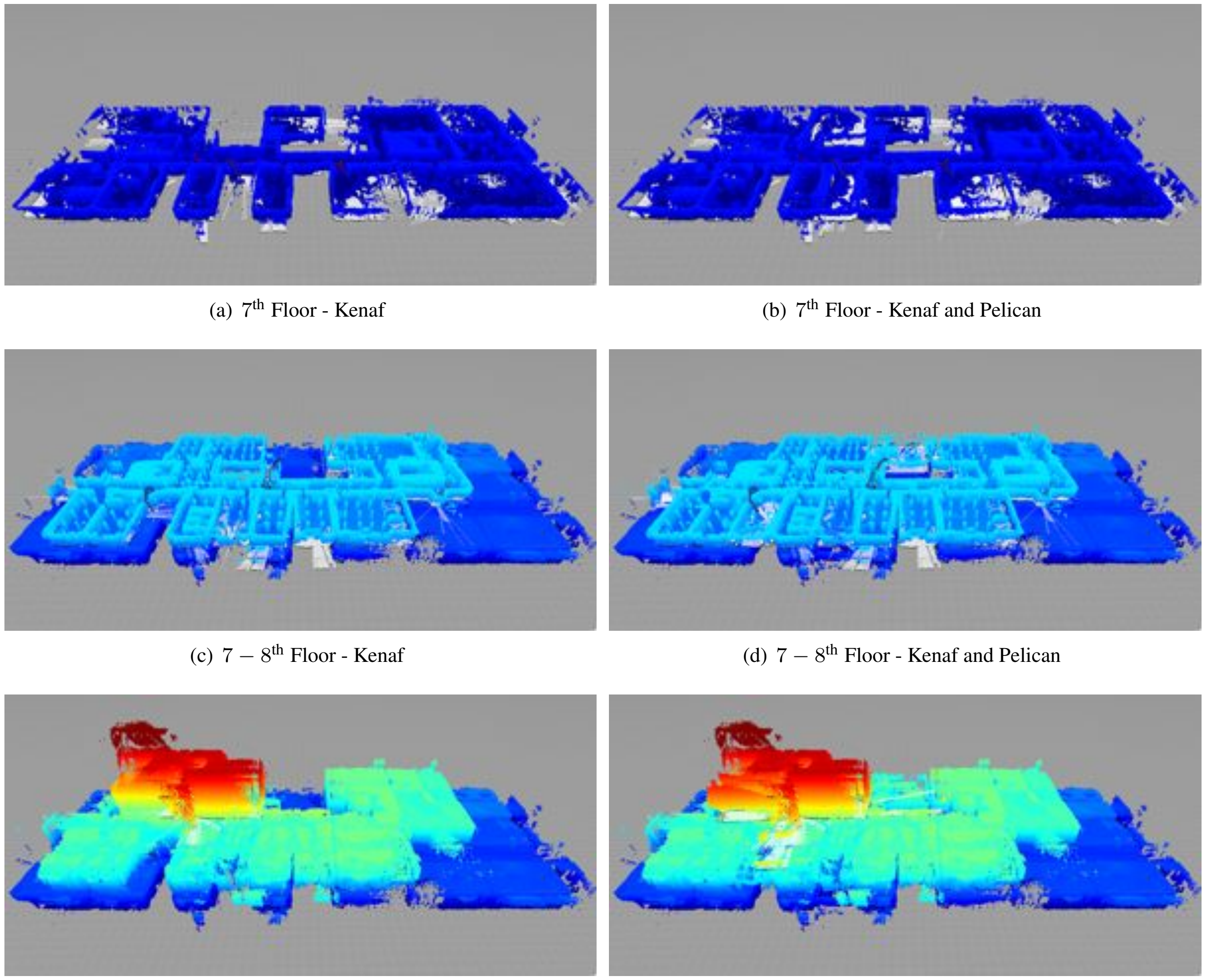

(a) 7th Floor - Kenaf

(b) 7th Floor - Kenaf and Pelican

(c) 7 – 8th Floor - Kenaf

(d) 7 – 8th Floor - Kenaf and Pelican

(e) 7 – 9th Floor - Kenaf

(f) 7 – 9th Floor - Kenaf and Pelican

Figure 11: The 3D voxel grid maps generated during the experiment. The map resulting from the Kenaf sensor data is shown on the left while the merged maps resulting from both the Kenaf and Pelican sensor data are shown on the right.

with a heterogeneous team of robots without any significant issues or failures is an encouraging argument that the technological level is close to applicable in real scenarios, there are still some fundamental challenges left to be addressed.

We must first acknowledge that the environment was modified prior to our entry in that it was cleaned of any hazardous materials and structural reinforcements were in place to prevent further building collapse. For this reason, one should be cautious to state that our experiments are completely representative of an earthquake-damaged building. However, the environment still possessed similar attributes to what one would expect: fallen beams, dust and debris throughout the interior, water pools where rain freely entered the building, wires hanging from the ceiling, and personal affects and furniture in disarray. Indeed, loose wall and ceiling materials were of concern for both the ground and aerial robots due to the possibility of breaking the vehicles. Many of the windows and walls were compromised, yielding inconsistent air flow that impacted the aerial robot's flight performance. Additionally, some of the debris and clutter proved to test the 2.5D assumption employed by the aerial robot to simplify the localization problem and permit real-time performance. Hence, we were not able to use the aerial robot in all locations that were inaccessible to the ground robot.

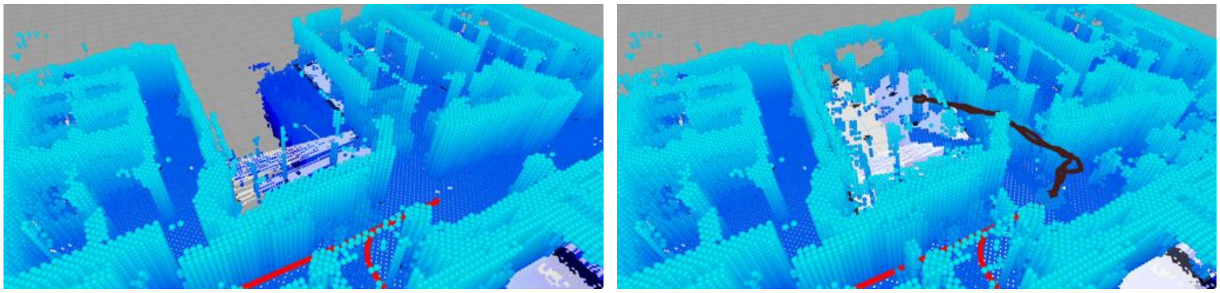

Figure 12: Merging the Kenaf and Pelican maps. The map generated by the Kenaf is shown on the left while the extended map via the Pelican observations along with the Quince and Pelican trajectories (red and black, respectively) are shown on the right.

In addition to the platform or algorithmic limitations, an interesting consideration that arose in this work is the role of autonomy for aerial robots in search and rescue. We found that tele-operation of an aerial robot can be quite challenging in complex and confined environments, particularly when the operator does not have direct line-of-sight and debris is interacting with the vehicle. An autonomous vehicle may be able to sense and locally avoid those external interactions and preserve stable flight while a tele-operated system may not yield the same result. We found this to be the case at several points during our experimentation when the operator failed to navigate the vehicle through tightly confined spaces but the fully autonomous vehicle was able to find a path and autonomously navigate through the confined space.

From these statements, one may conclude that areas that require the greatest attention in the future do not lie at the core problems of localization and mapping but more at the boundaries of these problem including the interfaces between the operators and the vehicles and vehicles and the environment. We require a better understanding of the appropriate methods to permit operators to interact with aerial robots in complex and confined environments such as those found in this work. Additionally, we must design aerial vehicles to be more robust to debris in the environment.

While there are still issues that must be addressed in the algorithms, these problems are primarily of pragmatic concern. At present, we require the 2.5D assumption on the aerial vehicle due to constrained onboard CPU capabilities. As CPUs becoming increasingly capable, we will continue to incorporate more sensor information and eliminate the need for the 2.5D assumption. We are particularly interested in eliminating this assumption in the near future as it is a major algorithmic limitation for the aerial platform. We are also interested in further experimentation with cooperative teams of ground and aerial robots but with multiple ground and aerial robots operating concurrently as opposed to the sequential phases in this work.

Acknowledgements

The authors gratefully acknowledge partial support from NSF Grant CNS-1138110, ARL Grant W911NF-08-2-0004, the JST J-RAPID program, and the NEDO Project for Strategic Development of Advanced Robotics Elemental Technologies.

References

Ackerman, E. (March 18, 2011). Japan Earthquake: iRobot Sending Packbots and Warriors to Fukushima Dai-1 Nuclear Plant. In *IEEE Spektrum*. Source: http://spectrum.ieee.org/automaton/robotics/industrial-robots/irobot-sending-packbots-and-warriors-to-fukushima.

Ascending Technologies, GmbH. Ascending Technologies, GmbH. http://www.asctec.de/.

Bachrach, A., Prentice, S., He, R., and Roy, N. (2011). RANGE - robust autonomous navigation in GPS-denied environments. *J. Field Robot.*, 28(5):644–666.

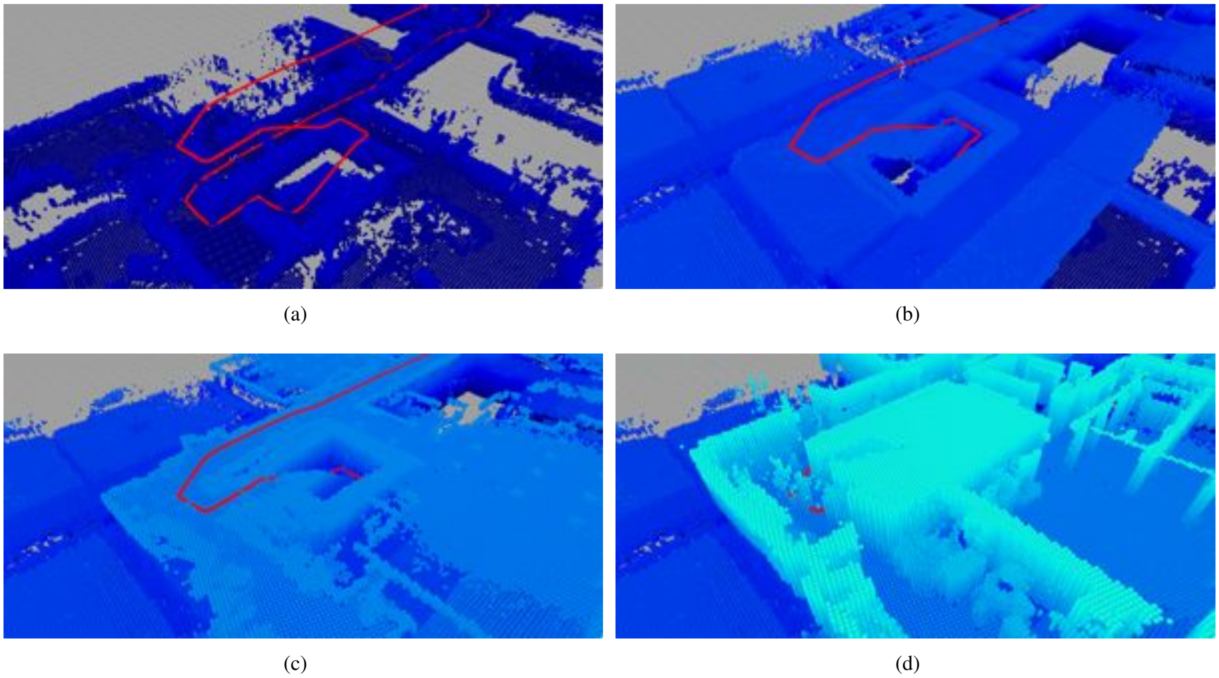

Figure 13: The 3D map generated for the stairwell traversed by the vehicles between the 7th and 8th floors showing various z-height levels of detail along with the trajectory followed by the Quince robot.

Gonzalez, F., Castro, M. P. G., Narayan, P., Walker, R., and Zeller, L. (2011). Development of an autonomous unmanned aerial system to collect time-stamped samples from the atmosphere and localize potential pathogen sources. *J. Field Robot.*, 28(6):961–976.

Guizzo, E. (August 23, 2011). Fukushima Robot Operator Writes Tell-All Blog. In *IEEE Spektrum*. Source: http://spectrum.ieee.org/automaton/robotics/industrial-robots/fukushima-robot-operator-diaries.

How, J. P., Fraser, C., Kulling, K. C., Bertuccelli, L. F., Toupet, O., Brunet, L., Bachrach, A., and Roy, N. (2009). Increasing autonomy of UAVs. *IEEE Robot. Autom. Mag.*, 16(2):43–51.

Kim, B., Kaess, M., Fletcher, L., Leonard, J., Bachrach, A., Roy, N., and Teller, S. (2010). Multiple relative pose graphs for robust cooperative mapping. In *Proc. of the IEEE Intl. Conf. on Robot. and Autom.*, pages 3185–3192, Anchorage, AK.

Magnitude (March 11, 2011). Magnitude 9.0 - near the east coast of Honshu, Japan. In *United States Geological Survey*. Source: http://earthquake.usgs.gov/earthquakes/eqinthenews/2011/usc0001xgp.

Michael, N., Shen, S., Mohta, K., Kumar, V., Nagatani, K., Okada, Y., Kiribayashi, S., Otake, K., Yoshida, K., Ohno, K., Takeuchi, E., and Tadokoro, S. (2012). Collaborative mapping of an earthquake-damaged building via ground and aerial robots. In *Proc. of the Intl. Conf. on Field and Service Robot.*, Matsushima, Japan.

Murphy, R., Kravitz, J., Stover, S., and Shoureshi, R. (2009). Mobile robot in mine rescue and recovery. *IEEE Robot. Autom. Mag.*, 16(2):91–103.

Nagatani, K., Kiribayashi, S., Okada, Y., Tadokoro, S., Nishimura, T., Yoshida, T., Koyanagi, E., and Hada, Y. (2011). Redesign of rescue mobile robot Quince - toward emergency response to the nuclear accident at fukushima daiichi nuclear power station on march 2011. In *Proc. of IEEE Intl. Sym. on Safety, Security, and Rescue Robotics*, pages 13–18, Kyoto, Japan.

Nagatani, K., Tokunaga, N., Okada, Y., and Yoshida, K. (2008). Continuous acquisition of three-dimensional environment information for tracked vehicles on uneven terrain. In *Proc. of the IEEE Intl. Workshop on Safety, Security, and Rescue Robot.*, Sendai, Japan.

Ohno, K., Kawahara, T., and Tadokoro, S. (2008). Development of a 3D laser scanner for measuring uniform and dense 3D shapes of static objects in dynamic environments. In *Proc. of IEEE Intl. Conf. on Robot. and Biomimetics*, pages 2161–2167, Bangkok, Thailand.

Ohno, K., Tadokoro, S., Nagatani, K., Koyanagi, E., and Yoshida, T. (2009). 3-D mapping of an underground mall using a tracked vehicle with four sub-tracks. In *IEEE Intl. Workshop on Safety, Security, and Rescue Robotics*, Denver, CO.

Ohno, K., Tadokoro, S., Nagatani, K., Koyanagi, E., and Yoshida, T. (2010). Trials of 3-D map construction using the tele-operated tracked vehicle Kenaf at Disaster City. In *Proc. of the IEEE Intl. Conf. on Robot. and Autom.*, pages 2864–2870, Anchorage, AK.

Okada, Y., Nagatani, K., Yoshida, K., Tadokoro, S., Yoshida, T., and Koyanagi, E. (2011). Shared autonomy system for tracked vehicles on rough terrain based on continuous three-dimensional terrain scanning. *J. Field Robot.*, 28(6):875–893.

Pellenz, J., Lang, D., Neuhaus, F., and Paulus, D. (2010). Real-time 3D mapping of rough terrain: A field report from Disaster City. In *Proc. of the IEEE Intl. Workshop on Safety, Security, and Rescue Robot.*, Bremen, Germany.

Pratt, K. S., Murphy, R. R., Burke, J. L., Craighead, J., Griffin, C., and Stover, S. (2008). Use of tethered small unmanned aerial system at Berkman Plaza II collapse. In *Proc. of the IEEE Intl. Workshop on Safety, Security, and Rescue Robot.*, Sendai, Japan.

Rohmer, E., Yoshida, T., Ohno, K., Nagatani, K., Tadokoro, S., and Koyanagi, E. (2010). Quince: A collaborative mobile robotic platform for rescue robots research and development. In *Intl. Conf. on Adv. Mechatronics*, pages 225–230, Osaka, Japan.

Shen, S., Michael, N., and Kumar, V. (2011). Autonomous multi-floor indoor navigation with a computationally constrained MAV. In *Proc. of the IEEE Intl. Conf. on Robot. and Autom.*, pages 20–25, Shanghai, China.

Shen, S., Michael, N., and Kumar, V. (2012). Autonomous indoor 3D exploration with a micro-aerial vehicle. In *Proc. of the IEEE Intl. Conf. on Robot. and Autom.*, Saint Paul, MN. To Appear.

Tabushi, H. (May 24, 2011). Company believes 3 reactors melted down in Japan. In *The New York Times*. Source: http://www.nytimes.com/2011/05/25/world/asia/25nuclear.html.